Texture evolution in CoCrPtTa/Cr/NiAl magnetic recording media

B. Lu,[a] D. E. Laughlin, and D. N. Lambeth
Data Storage System Center, Carnegie Mellon University, Pittsburgh, Pennsylvania 15213

S. Z. Wu, R. Ranjan, and G. C. Rauch
Seagate Technologies, Recording Media Group, 47010 Kato Road, Fremount, California 94538

Crystallographic textures in a CoCrPtTa/Cr/NiAl multilayer magnetic recording media were studied by electron diffraction. It was found that texture quality evolves through the thickness of the films. A large improvement of texture quality was discovered at the interface of the Cr and NiAl layers. Surprisingly, there remains a portion of randomly oriented grains in the CoCrPtTa layer, in addition to the anticipated grains of $[10\bar{1}0]$ texture. The texture quality of the CoCrPtTa layer remains similar to that of the underlying Cr layer. © *1999 American Institute of Physics.* [S0021-8979(99)50108-4]

I. INTRODUCTION

Co-alloy/Cr/NiAl and Co-alloy/Cr are two major configurations of the multilayers (magnetic layer/intermediate layer/underlayer) adopted by the rigid disk industry.[1] The first set has many advantages over the latter as far as the issues of noise and thermal stability are concerned. The sputtered NiAl grain size is more uniform and can be as small as one half of that of Cr grains,[2] therefore, smaller Co-alloy grains can be obtained. Because of the orientation differences, the lattice match between the three layers in the first configuration is much better than the latter.[3] As a result, there are less structural defects in the magnetic layer, which allows the Co grains to achieve their maximum magnetocrystalline anisotropy. Moreover, in the latter configuration, the exchange coupling between the bicrystals within a Co-alloy $(11\bar{2}0)$ grain results in a reduction of the effective anisotropy.[4]

Crystallographic textures developed in an underlayer and transferred to the magnetic layer can be very poor. Since the magnetic properties are strongly influenced by the quality of the texture, it is more important to know the quality of the preferred orientation (PO) rather than to simply know what the PO is.

In this article, we have used electron microscopy techniques to study the texture evolution at different positions through the thickness of a CoCrPtTa/Cr/NiAl multilayer sputtered on NiP/Al–Mg substrates by production processes. A tilting electron diffraction technique[5,6] was used to quantitatively evaluate the texture quality for each layer. The textures of each layer are compared and discussed in detail. The purpose of this study is to clarify the evolution of the Cr [112], NiAl [112], and the CoCrPtTa $[10\bar{1}0]$ textures through the thin-film thickness.

II. EXPERIMENT

Thin films of CoCrPtTa (200 Å)/Cr (700 Å)/NiAl (940 Å) were sputter deposited at room temperature using an Intevac MDP 250B deposition system. TEM specimens were mechanically polished from the back (substrate side) of the sample. Subsequently, they were ion milled from the back on a liquid N_2 stage of a Gatan 600 ion miller using a single Ar ion gun. A Gatan 691 precision ion polishing system (PIPS) was used to ion polish the specimen for 5 min at room temperature. This method of specimen preparation allows for the observation of the CoCrPtTa layer at the edge of the TEM sample.

After the first electron diffraction (ED) experiments, the specimen was further ion polished from the front of the specimen to remove the magnetic layer. By carefully controlling the ion polishing parameters, the Cr layer could be revealed at the edge of the specimen. Then, ED was carried out on only the Cr layer. Subsequently, the specimen was ion polished to remove the Cr layer, and the remaining NiAl layer was analyzed.

III. RESULTS AND DISCUSSIONS

Figures 1(a)–1(f) are a series of tilted electron diffraction patterns of the NiAl underlayer. The specimen was tilted around the direction shown by the long arrow marked with ''OT'' in Fig. 1(f). The arrow marked with ''OF'' shows the direction that the specimen was tilted away from the 0°-tilt EDP [Fig. 1(a)]. Superlattice rings $[h+k+1=2n+1$, indexed in Fig. 1(c)] can be seen in each of the six EDPs. These are due to the $B2$ structure of the NiAl crystal. It is interesting to note in Fig. 1(a) that the {100}, {200}, and {400} rings are not present in the 0°-tilt pattern, while other rings including the superlattice rings, such as {110}, {111}, {210}, {211}, {220}, {221}, {310}, {311}, {222}, {320}, and {321} can be observed with different intensities. These patterns are consistent with a weak NiAl [112] texture, in which the [112] orientations of NiAl grains are not all exactly parallel to the film normal but make a distribution inside a large solid angle around the film normal. The texture axis distribution angle (α) is defined as the angle between the surface normal and the edge of the distribution cone. Similar to the PW50 of an x-ray rocking curve, the larger the texture axis distribution, the worse the texture quality. Therefore, the texture axis distribution angle (α) can be used to evaluate the texture quality.

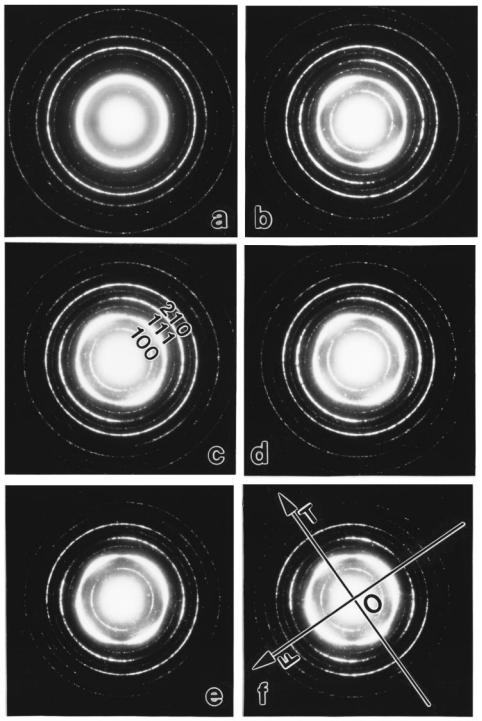

FIG. 1. Electron diffraction patterns (EDPs) of the NiAl layer. The EDPs are taken at different tilt angles around the tilt axis OT: (a) 0°, (b) 38°, (c) 41°, (d) 44°, (e) 50°, and (f) 56°.

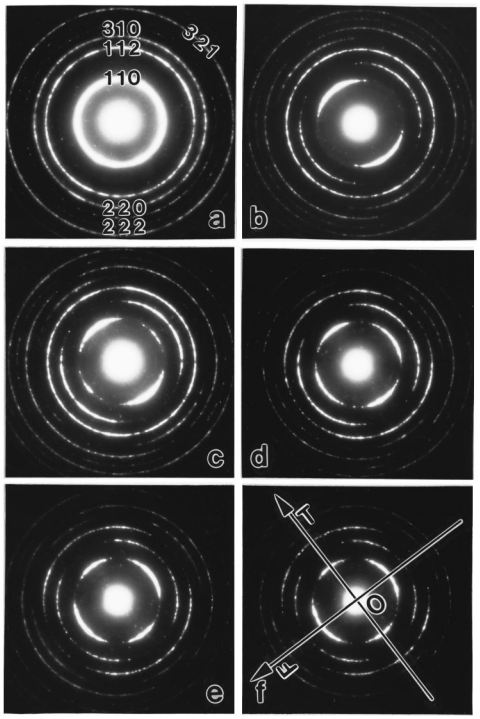

FIG. 2. EDPs of the Cr layer. The EDPs are taken at different tilt angles around the tilt axis OT: (a) 0°, (b) 29°, (c) 37°, (d) 45°, (e) 52°, and (f) 55°.

The observed rings in Fig. 1(a) can be divided into two categories: (1) those perpendicular to the [112] texture axis, and (2) those not perpendicular to the texture axis. The rings {110}, {111}, {210}, {220}, {311}, {222}, and {321} fall into the first category, while the rings {211}, {221}, {310}, and {320}, which have angles with [112] of 80.4°, 82.2°, 82.6°, and 83.5°, respectively, belong to the second category. The presence of the nonperpendicular rings suggests that the texture axis distribution angle (α) is larger than $90° - 80.4° = 9.6°$. As a result, all the rings appear as belts, which are wide enough for the {211}, {221}, {310}, and {320} rings to intersect the Ewald sphere. Consequently, these rings appear on a 0°-tilt EDP. The logic behind the missing $\{h00\}$ rings is that the largest angle between the $\{h00\}$ and the [112] direction is 65.9°, which means that the $\{h00\}$ belts are too far from the Ewald sphere to be shown in a 0°-tilt EDP. This indicates that the distribution angle α is smaller than $90° - 65.9° = 24.1°$.

Based on the results of x-ray θ–2θ diffraction scan curves, previous studies[7] have shown that both [110] and [112] POs exist in the same NiAl layer deposited on a glass substrate. Here, the absence of ED $\{h00\}$ rings confirms that there is only the [112] PO existing in the studied NiAl layer sputtered on the NiP/Al–Mg substrate. However, we cannot rule out the existence of some [110] PO at the NiAl/NiP interface.

As the specimen is tilted away from the 0°-tilt position, the rings present in Fig. 1(a) become arcs. The rings which are perpendicular to the texture axis show arcs along the tilt axis, OT, while the nonperpendicular rings' arcs stay along the forward direction, OF. As the tilt angle increases, the arc along OT become smaller, but the arc along OF first increases then splits into two. This can be easily understood in terms of the texture dispersion. For the same tilt angle, the shorter the OT arc, the smaller the α, and the sooner the OF arc splits, the smaller is α. The relationship between the texture axis distribution angle, tilting angle, and the arc degree is[5] $\sin(\omega_0/2) = \sin\alpha/\sin\beta$, for a given OT arc. Here, 1 ω_0 is the arc degree, α is the texture axis distribution angle, and β is the tilt angle. Therefore, by plotting $\sin(\omega_0/2)$ vs $1/\sin\beta$ for an OT arc, $\sin\alpha$ can be obtained as the slope of the line. Consequently, α can be determined.

Figures 2(a)–2(f) show a tilting series of EDPs of the Cr layer. Because of the bcc structure of the Cr crystal, only the reflections with the condition $h+k+1=2n$ appear, as indexed in Fig. 2(a). Again, due to the [112] texture of the thin film, the {200} and {400} rings are not present in the 0°-tilted pattern [Fig. 2(a)]. The {112} and {310} rings, which make angles of 80.4° and 82.6° with the texture axis, respectively, also appear in Fig. 2(a). By the same reasoning as discussed for the NiAl layer, the value of the texture axis distribution angle α is between 9.6° and 24.1°. By comparing Figs. 1 and 2, it can be seen that the {110} arcs of Cr are shorter than those of NiAl at nearly the same tilting angle. Also, the {200} arcs of Cr each break into two sooner than those of NiAl. These effects demonstrate that the Cr layer has a stronger [112] texture than the NiAl layer.

Figures 3(a)–3(f) are a tilting series of EDPs of both the CoCrPtTa and Cr layers. Because the CoCrPtTa layer is only 200 Å thick, electron diffraction was carried out on both the CoCrPtTa layer and the top part of the Cr layer.

From the 0°-tilt EDP [Fig. 3(a)], it can be seen that the $\{10\bar{1}0\}$, $\{10\bar{1}1\}$, and $\{10\bar{1}2\}$ rings whose largest angles

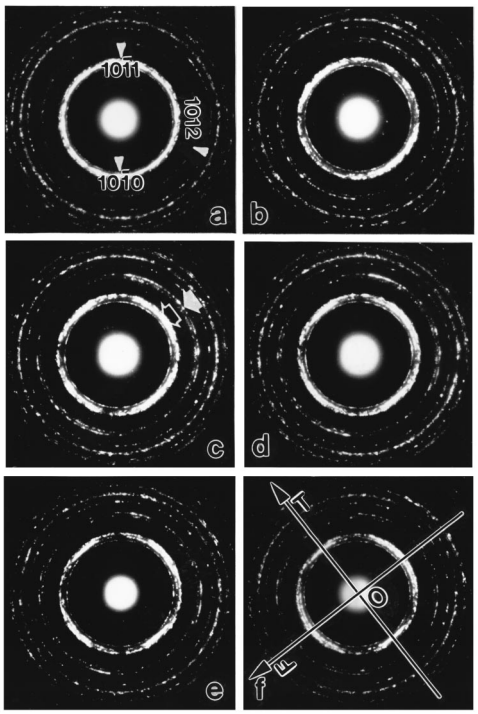

FIG. 3. EDPs of the CoCrPtTa and Cr layers. The EDPs are taken at different tilt angles around the tilt axis OT: (a) 0°, (b) 29°, (c) 38°, (d) 41°, (e) 44°, and (f) 50°.

from the $[10\bar{1}0]$ direction are 60°, 63.8°, and 70.0°, respectively, are present. These rings of $[10\bar{1}0]$ texture are too far from the Ewald sphere to appear on the EDP. Hence, they must originate from randomly orientated crystalline grains in the CoCrPtTa layer. The CoCrPtTa (0002) and Cr (110) ring overlap and lie between the $\{10\bar{1}0\}$ and $\{10\bar{1}1\}$ rings.

As the specimen is tilted away from the 0°-tilt position, the CoCrPtTa(0002)/Cr(110) ring begins to shrink along the OT axis. At the same time, the Cr {200} arcs and the arcs from the nonperpendicular Cr {110} rings start to appear along the OF direction as shown in Fig. 3(c) (solid and open arrow, respectively). The effect of texture on the CoCrPtTa rings is not as strong as that on the Cr rings, due to the portion of randomly oriented grains. However, the effect of texture can still be observed via the intensity variation of the $\{10\bar{1}0\}$ and $\{10\bar{1}1\}$ rings. In spite of the background intensity, caused by the randomly oriented grains, the $\{10\bar{1}0\}$ ring appears to be two arcs along OF in Fig. 3(b), and each splits into two in Figs. 3(c) and 3(d). The intensity change of the $\{10\bar{1}1\}$ ring is also consistent with a $[10\bar{1}0]$ texture.

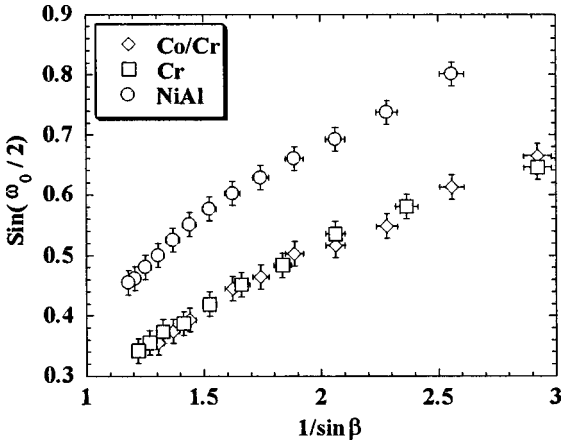

FIG. 4. Plots of $\sin(\omega_0/2)$ vs $1/\sin\beta$ of the three layers.

Figure 4 shows plots of $\sin(\omega_0/2)$ vs $1/\sin\beta$ for the three EDP series in Figs. 1, 2, and 3. The data were collected based on the OT arcs of NiAl {110}, Cr {110}, and CoCrPtTa {0002}/Cr {110} from the three sets of EDPs. The texture axis distribution angles of the CoCrPtTa/Cr, Cr, and NiAl layers were determined to be 10.8°, 10.6°, and 14.4°, respectively.

Therefore, the [112] orientations of the NiAl grains are more dispersed around the surface normal than the [112] orientations of Cr grains and $[10\bar{1}0]$ orientations of CoCrPtTa grains. In other words, the use of a Cr intermediate layer improves the texture quality of the CoCrPtTa layer over what would be anticipated without the use of the Cr layer.

ACKNOWLEDGMENTS

This work was support by Intevac and by the Data Storage System Center of Carnegie Mellon University. The U.S. Government is authorized to reproduce and distribute reprints for governmental purposes notwithstanding any copyright notation thereon.

[1] M. Mirzamaani, X. Bian, M. F. Doerner, J. Li, and M. Parker, IEEE Trans. Magn. **34**, 1588 (1998).
[2] L.-L. Lee, D. E. Laughlin, and D. N. Lambeth, IEEE Trans. Magn. **30**, 3951 (1994).
[3] D. N. Lambeth, W. Yang, H. Gong, D. E. Laughlin, B. Lu, L.-L. Lee, J. Zou, and P. S. Harllee, Mater. Res. Soc. Symp. Proc. (to be published).
[4] Q. Peng, H. N. Gertram, N. Fussion, M. Doerner, M. Mirzamaani, D. Margulies, R. Sinclair, and S. Lambert, IEEE Trans. Magn. **31**, 2821 (1995).
[5] L. Tang and D. E. Laughlin, J. Appl. Crystallogr. **29**, 411 (1996).
[6] L. Tang, Y. C. Feng, L.-L. Lee, and D. E. Laughlin, J. Appl. Crystallogr. **29**, 419 (1996).
[7] L.-L. Lee, D. E. Laughlin, and D. N. Lambeth, IEEE Trans. Magn. **MAG-31**, 2728 (1995).